Available online at www.sciencedirect.com

ScienceDirect

journal homepage: www.elsevier.com/locate/bbe

Original Research Article

Fast, accurate and robust retinal vessel segmentation system

*Zhexin Jiang, Juan Yepez, Sen An, Seokbum Ko**

University of Saskatchewan, Department of Electrical and Computer Engineering, Saskatoon, Canada

ARTICLE INFO

Article history:
Received 13 December 2016
Accepted 9 April 2017
Available online 19 April 2017

Keywords:
Retinal images
Vessel segmentation
Morphological processing
DoOG filter
Automated analysis
Thresholding

ABSTRACT

The accurate segmentation of the retinal vessel tree has become the prerequisite step for automatic ophthalmological and cardiovascular diagnosis systems. Aside from accuracy, robustness and processing speed are also considered crucial for medical purposes. In order to meet those requirements, this work presents a novel approach to extract blood vessels from the retinal fundus, by using morphology-based global thresholding to draw the retinal venule structure and centerline detection method for capillaries. The proposed system is tested on DRIVE and STARE databases and has an average accuracy of 95.88% for single-database test and 95.27% for the cross-database test. Meanwhile, the system is designed to minimize the computing complexity and processes multiple independent procedures in parallel, thus having an execution time of 1.677 s per image on CPU platform.

1. Introduction

The retinal vasculature has been acknowledged as an indispensable element in both ophthalmological and cardiovascular disease diagnosis such as glaucoma and diabetic retinopathy. The attributes of retinal blood vessels including length, width, tortuosity, branching pattern and angles will contribute to the diagnostic result. However, manual segmentation of retinal blood vessels, although possible, is a time consuming and repetitive work, and it also requires professional skills. To assist ophthalmologists with this complex and tedious work, the demand for the fast automated analysis of the retinal vessel images arises.

However, to fully automate the analysis and make it work for real-life diagnosis is a harsh task. First, because even the thinnest vessel may contribute to the differential diagnosis list, in order to avoid medical accidents, the extraction of blood vessels is required to be extremely accurate so as to help the diagnosis. Second, for many diseases such as diabetes and hypertension, patients are required to take regular ocular screening in order to detect retinopathy in early stages. However, patients who are inconvenient to move or live distantly from the city will be less approachable for the location-specific treatment. In this case, the automated solution is expected to be handy and portable in the future. Besides, almost every retinal vasculature extraction system is facing the trade-off between accuracy and computing

* *Corresponding author at:* University of Saskatchewan, Department of Electrical and Computer Engineering, 57 Campus Drive, Saskatoon, Canada S7N 5A9.
E-mail address: seokbum.ko@usask.ca (S. Ko).
http://dx.doi.org/10.1016/j.bbe.2017.04.001

complexity. What's more, even though some algorithms have achieved a decent accuracy within a certain database, but they do not necessarily provide or maintain the similar performance over the cross-database test.

In an attempt to provide a fast, accurate and robust automatic segmentation, this paper proposes an innovative segmentation system that tries to solve the above problems. In recent researches, the most popular approaches for automated vessel segmentation are supervised methods, matched filtering, and morphological processing, while the proposed system combines both matched filtering and morphological processing together not just to achieve higher accuracy and better robustness, but also to decrease the computing complexity and shorten the execution time.

The organization of the paper is as follows. Section 2 will describe related works and introduce three basic approaches that have been applied to the proposed system and their contributions to this work. Section 3 will demonstrate the complete design of the proposed system including its workflow and function of every block. Section 4 will present the performance measurement on three aspects and compare with other works. Section 5 will conclude the paper and point out the future research direction.

2. Background

The proposed system is enlightened by numerous previous works and consists of several classic methods. This section will briefly cover the existing retinal vessel segmentation approaches and then introduce the principle and strength of the proposed system.

2.1. *Related works*

According to Fraz's survey [1], the existing retinal segmentation techniques on 2-D retinal images can be summarized into six categories; (i) pattern recognition, (ii) mathematical morphology, (iii) matched filtering, (iv) vessel tracking, (v) model based approaches and (vi) parallel/hardware approach, among which pattern recognition contributes to most of the accurate and robust works, while parallel/hardware methods accelerate the execution speed with a relatively lower accuracy [2,3]. (ii), (iii), (iv) and (v) contain the basic techniques that cooperate with each other or apply to (i) and (vi) to form an automated vessel segmentation system.

Pattern recognition based algorithms, dealing with the automated detection or classification of the retinal blood vessel and non-vessel features, are divided into supervised methods such as Refs. [4–8] and unsupervised approaches such as Ref. [9]. In supervised methods, the rule for vessel extraction is trained by the algorithm on the basis of manually segmented images by ophthalmologists. As supervised methods are developed with the reference of the gold standard dataset, their performance is usually better than that of the unsupervised ones. However, because such classified ground truth data will not be available in real life applications, a supervised algorithm thus shall be trained and tested over different databases to assess its robustness. The unsupervised classification methods intend to find inherent patterns of retinal vessels within images for deciding whether a particular pixel is part of the vessel or not.

Mathematical morphology containing a set of image processing techniques is one of the most famous approaches for image segmentation. It extracts image components that are useful while smoothing the rest area. The morphological operation has the advantage of speed and noise resistance in identifying specific shapes such as features, boundaries, skeletons and convex hulls, by applying structuring elements (SE) to greyscale or binary images [10–13].

Matched filtering techniques usually convolve a 2-D kernel (or structural element) for blood vessel cross-profile identification (typically a Gaussian or Gaussian-derivative profile). The kernel is rotated into many different directions to model a feature in the image at some unknown position and orientation, and the matched filter response (MFR) indicates the presence of this feature. Such techniques are very effective to detect vessel centerlines [10,14,12].

In most cases, vessel tracking algorithms are more effectively used in conjunction with matched filters of the morphological operators, such as Refs. [14] and [15]. Tracking a vessel means to follow the vessel centerline guided by local information and try to find the path which best matches a vessel profile model, through which not only the centerline but also the widths of each individual vessel will be accurately extracted.

Model-based approaches such as vessel profile models in Ref. [16], extracting retinal vessels by using explicit vessel models, are designed to handle both normal and pathological retinas with bright and dark lesions simultaneously. Some other methods using deformable models such as parametric models and geometric models are not as effective as the former one.

2.2. *Methodology*

In this work, mathematical morphology and matched filtering are applied to the proposed vessel segmentation system. During the processes, the retinal images shall firstly be transformed into greyscale and then go through the top-hat transform, intensity thresholding and centerline highlighting, which will be briefly discussed in this subsection.

2.2.1. *Morphology processing*

Two operations belonging to the mathematical morphology (MM) theory will be applied to the proposed system, which is top-hat transform and morphology erosion. The top-hat method is utilized to redistribute the greyscale intensity from a preprocessed greyscale retinal image, in order to generate a characteristic feature for vessel/non-vessel classification, while the erosion operation helps to de-noise the image and smooth the vessel edges in the final post-processing stage.

The principle of morphology processing is to simplify the image data through retaining their essential characteristics from a shape and removing other extraneous elements. The basic operations in MM processing are erosion, dilation, opening, and closing, which deduce the top-hat transform — one of the most efficient way to do feature extraction, background equalization, and image

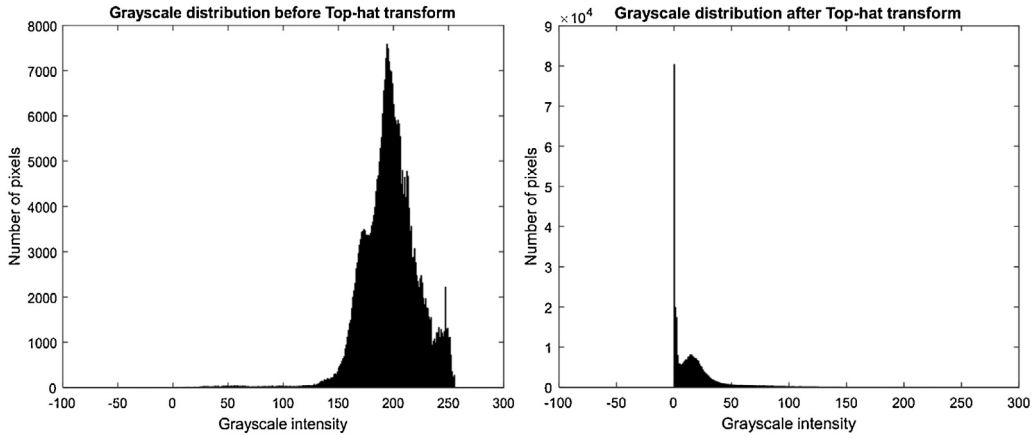

Fig. 1 – Different greyscale distribution before (left) and after (right) the top-hat transform.

enhancement. The mathematical definitions of a white top-hat transform can be formulated as Eq. (1),

$$T_W(f) = f - f \circ b \tag{1}$$

where f is a greyscale image; b is a greyscale structuring element; the symbol $\circ$ denotes the opening operation; T_W denotes the white top-hat transform, where the object elements are highlighted brighter than their surroundings.

Since the top-hat transform is sensitive to ridges and peaks (the sharp changes in greyscale intensity values), when provided with a preprocessed greyscale retinal vessel image, it will be capable of highlighting the vessel structure while smoothing the rest non-vessel background in different illumination conditions, by considering the edges of vessels as peaks and the flat fundus as the background. However, not just vessels but also noises (such as non-vessel tissues) are likely to be introduced into the results during this process. To solve this, the proposed solution will be discussed in Section 2.2.2.

Once top-hat transform is completed, the intensity is reconstructed into another distribution. A demonstration of intensity changes before and after the transform is given in Fig. 1,

where about 87% pixels have the intensity of 0 after redistribution. Meanwhile, a small gap could be visually speculated in the right histogram between intensity value 0 and 25, implying there exists a possible threshold to distinguish the vessel/non-vessel pixels. According to this, the greyscale intensity is selected as the characteristic feature for vessel classification, assuming that most non-vessel pixels have intensity value close to 0.

On the other hand, the algorithm of MM theory is born with parallel implementation structures, thus preserving the possibility to accelerate the processing speed with multi-threading, which will be presented in Section 4.

2.2.2. *Intensity thresholding*

Image thresholding enjoys a central position in applications of image segmentation, because of its intuitive properties, the simplicity of implementation and computational speed. The proposed system will utilize global intensity thresholding after the top-hat reconstruction of the greyscale image, through which a binary image will be generated according to Eqs. (2) and (3),

$$g(x,y) = \begin{cases} 1, & \text{if } f(x,y) > T \quad (2) \\ 0, & \text{if } f(x,y) \le T \quad (3) \end{cases}$$

where $f(x, y)$ corresponds to the input image and $g(x, y)$ represents the binary image after thresholding. Any point (x, y) in the image at which $f(x, y) > T$ is recognized as an object point, or vessel element; otherwise, the point is regarded as a background point, or non-vessel element. The threshold value T in this system is an empirical threshold, rather than using approaches like Otsu's method to generate one. The reason behind this mainly owing to small vessels are very thin structures, they usually present low local contrast and hard to be distinguished with their surrounding noises (or non-vessel tissues). In this case, the vessel segmentation process is divided into two phases: the venules structure extraction and the capillary detection. For the venules segmentation, there will not require an optimal threshold to classify the distribution, but a more ''strict'' threshold (larger than optimal) to eliminate the noises while sacrificing some certain thin vessels, in order to achieve a higher positive predictive value (PPV). But at the same time, another different method will be specifically utilized for capillary detection as a complement.

2.2.3. *Centerline highlighting*

Because both venules and capillaries are crucial for ophthalmological diagnosis, and the venules segmentation process intends to have ignored most of the thin vessels, in this case, capillaries need to be retrieved through centerline detection. Because of the fineness of capillaries, the centerline of a thin vessel can be used to approximate itself, thus completing the function of a vessel extraction system.

Centerline highlighting is the preliminary but the most important step for capillaries detection. It intends to highlight the candidate pixels which could possibly be the ridges of the vessels, by applying a first-order derivative filter orthogonally to the main orientation of the vessel. In this case, derivative values with opposite signs will be obtained on both hillsides

of the vessel. In other words, there will be positive values on one side of the vessel cross section while negative values on the other, by which a sign matrix will be obtained. Since the opposite signs indicate two hillsides of a vessel, the presence of centerline thus can be reflected by just scanning for the sign formats. After the pixels of a centerline were located, the intensity value of them will be replaced by the summation of the absolute values of the two horizontal neighbor pixels, in order to highlight the centerline. A particular kernel is proposed here which is the difference of offset Gaussians (DoOG) filters. DoOG filter is famous for its peak sensitivity and noise resistance, shown in Eq. (4).

$$\begin{bmatrix} -1 & -2 & 0 & 2 & 1 \\ -2 & -4 & 0 & 4 & 2 \\ -1 & -2 & 0 & 2 & 1 \end{bmatrix} \tag{4}$$

However, because the above process only works for the vertical direction, the image itself or the kernel must be rotated in order to be performed in all directions, and this will be discussed in the next section. The idea of centerline highlighting is from the work of Refs. [10] and [12].

3. Proposed system

The proposed vessel segmentation system can be schematically described by the functional block diagram as shown in Fig. 2, where we identify four main processing phases.

In the first preprocessing phase, the goal is to transform the input (RGB image) into greyscale, which will be the input for both venules structure segmentation and capillaries detection phases. As mentioned earlier, since most retinal images have a variational grey level contrast, and the contrast between capillaries and noises is closer than those with venules, this system thus proposes two parallel branches, which focus on different scale to segment venules and capillaries separately. The last stage will overlap and de-noise the results from the previous phases in order to create an image with a clear vascular structure and abundant thin vessels.

3.1. *Preprocessing*

To provide a greyscale output with great contrast, the proposed preprocessing will firstly remove the "black ring" and replace it with the color of the average level of the fundus background (see Fig. 3(b)). In order to get the average level of the background, three random areas ($50 \times 50 \times 3$ matrix) inside the fundus will be selected and the mean value of these matrixes will be calculated. This procedure creates the uniformity of the background and it is quite important for the top-hat transform because a more balanced background will improve the quality of segmenting the object elements. After replacing the black ring, the optimized RGB image will be transformed into greyscale through green channel (see Fig. 3 (c)), which has been considered in several works [4,17], as it naturally presents a higher contrast between vessels and fundus background.

3.2. *Venules structure extraction*

The object for venules structure extraction is to extract large vessels as much as possible, but leave the small ones to capillaries detection. Based on the work of preprocessing,

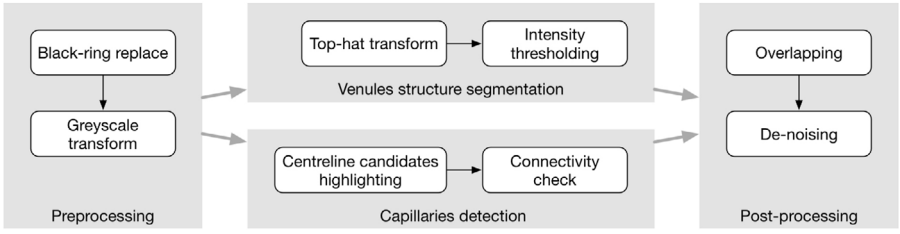

Fig. 2 – Functional diagram of the proposed retinal vessel segmentation system.

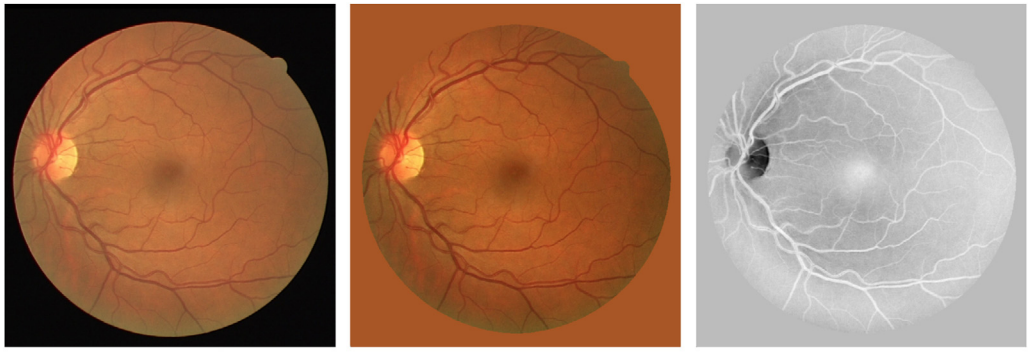

Fig. 3 – Preprocessing phase: (a) original RGB image; (b) RGB image after black ring removal; (c) greyscale image after transform through green channel.

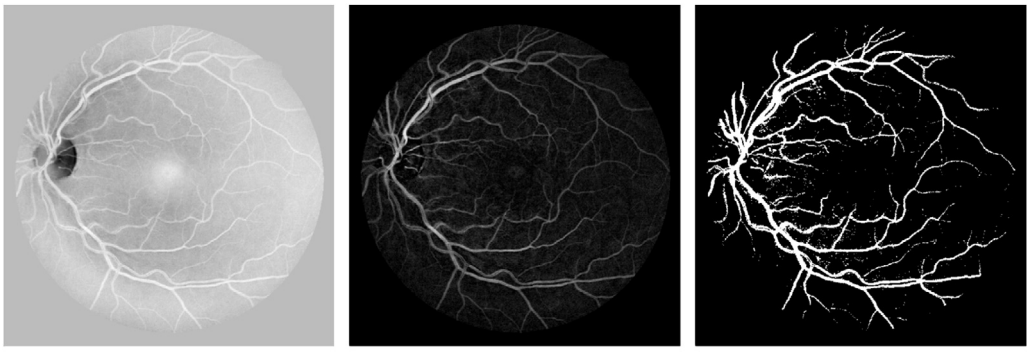

Fig. 4 – Venules structure extraction phase: (a) image after preprocessing; (b) image after top-hat transform; (c) image after intensity thresholding.

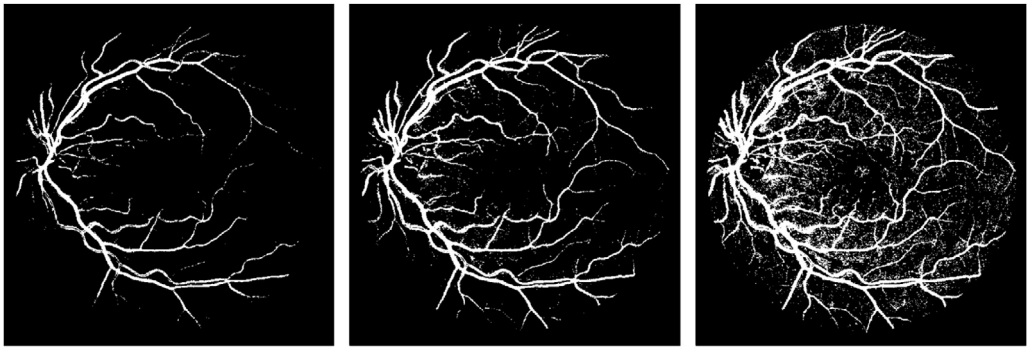

Fig. 5 – Comparison with different thresholds: (a) intensity thresholding with very a strict threshold; (b) intensity thresholding using proposed threshold; (c) intensity thresholding with a loose threshold.

the first step in this stage is to directly perform top-hat transform (see Fig. 4(b)). However, many other retinal tissues such as the optic disc, macula, fovea, and posterior pole will become the noises as they have a relatively close contrast to vessels. To eliminate these noises, the global intensity thresholding is used here. It classifies vessel and non-vessel elements with minimum computing complexity. Fig. 4(c) shows a clear vessel skeleton after thresholding.

To find a proper threshold, there are various approaches such as adaptive thresholding and Otsu's method, but here the system proposes a fixed empirical threshold. Generally speaking, the adaptive thresholding method usually generates a different threshold for each individual image to best fit its own intensity distribution, but such methods simply increase computing complexity because the system has to learn the strategy to analyze the image and to make decisions. For approaches like Otsu's method, aiming to find the best barrier to differentiate the intersected intensity classes, is not ideal for segmenting retinal blood vessels. Because the non-vessel tissues become very similar after being filtered by green channel during the preprocessing phase. In this case, the Otsu's method in retinal vessel segmentation will be more likely to preserve those unwanted non-vessel tissues and preform similarly to a loose threshold (see Fig. 5(c)). Therefore, a more strict threshold than the Otsu's optimal one is proposed for this system, to reduce most noises while sacrificing thin vessels. Fig. 4 shows the entire process of the current phase and Fig. 5 provides the comparison of results using three different thresholds.

3.3. *Capillaries detection*

While extracting venules structure, capillaries detection will also be running simultaneously with the same input image. But the input image needs to be black-and-white reversed (see Fig. 6(b)) in order to maintain the consistency, for the result after this phase shall be the vessel in white and background in black.

As mentioned previously, the most important step of detecting centerline pixels is applying the first-order derivative filter (given in Eq. (4)) orthogonally to the main orientation of the vessel centerline in all directions. To enable the detection in all directions, the image itself will be rotated instead of rotating the kernel in avoid of losing image information. The results after each rotation will be combined into one to realize the complete coverage of every direction. During the experiment, we found the best rotation step is 10 degrees (18 directions) for preserving most capillaries while

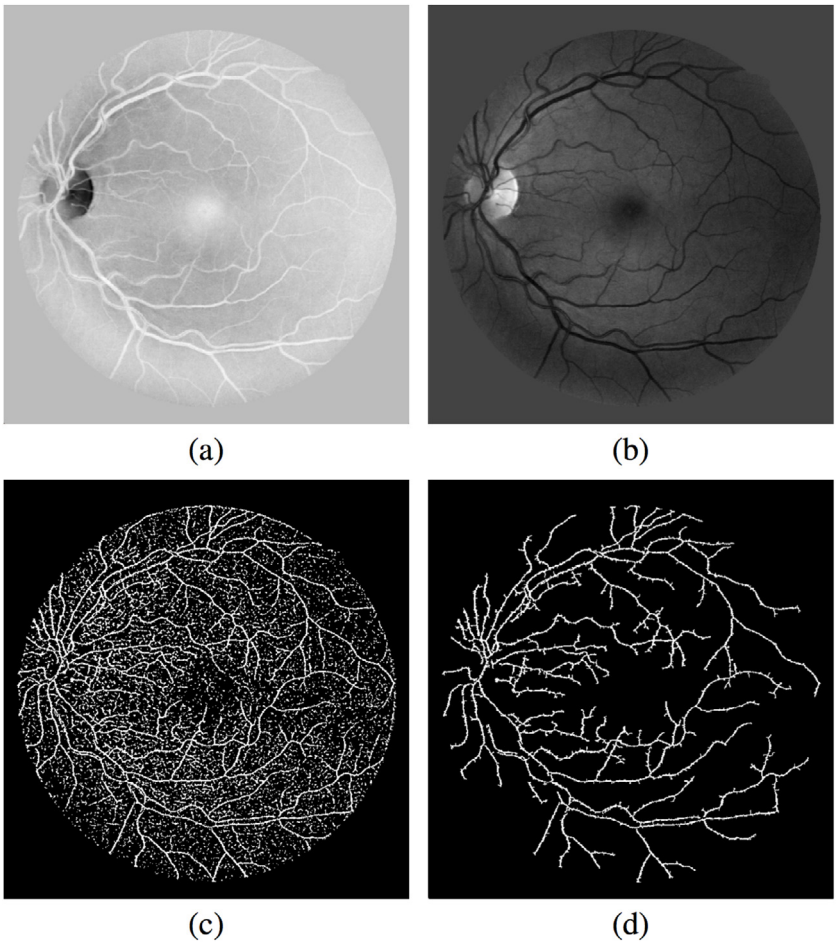

Fig. 6 – Capillaries detection phase: (a) image after preprocessing; (b) image after black-and-white inversion; (c) image after centerline highlighting; (d) the final result of capillaries detection after connectivity test.

maintaining a good running time. Thus, this entire process can be simply regarded as processing 18 different images and overlapping their results, while the process of each iteration has already been explained in Section 3.2. Fig. 6(c) shows the result of centerline highlighting.

The second part of capillaries detection is to eliminate the centerline candidates that have low connectivities. The connectivity between the current pixel and every of its surrounding neighbors will be examined. If connected, they will be categorized into the same group. When the examination for every pixel is done, the groups with its member size smaller than a fixed empirical threshold value will be removed. The smaller the threshold is, the more details it preserves, but a smaller threshold also increases the risk of keeping noises, thus pushing more pressure to the de-noising part. On the other hand, although larger threshold may bring in the risk of removing necessary capillary fragments, but it will eliminate more noises. Besides, capillary fragments can hardly have any scientific value in real situation and that is why this system proposes a fairly larger threshold for connectivity check. Fig. 6 (d) shows the final result after connectivity test and Fig. 6 presents the whole process of capillaries detection.

3.4. *Post-processing*

The final stage of retinal vessel segmentation is post-processing, which contains image overlapping and morphology de-noising. The word ''overlapping'' here means to combine the venules structure image (see Fig. 4(c)) and capillaries image (see Fig. 6(d)) into one, by simply applying the logic OR operation to both of them. The result is shown in Fig. 7(c)).

After overlapping, some noises which have been existing since venules structure extraction was accomplished need to be removed. The reason to keep these noises until the overlapping phase is because the noises may be overlapped or reconnected with vessel centerlines to enhance the vessels.

The overlapped image will be de-noised by applying erosion operation from the MM theory. Erosion operation has the ability to shrink the edge of the larger object and remove small spots, and in this way, not just the coarse edges of the vessels will be polished but also the scattering noises will be removed. Fig. 7(d) shows the final result after de-noising and Fig. 7 presents the entire post-processing process.

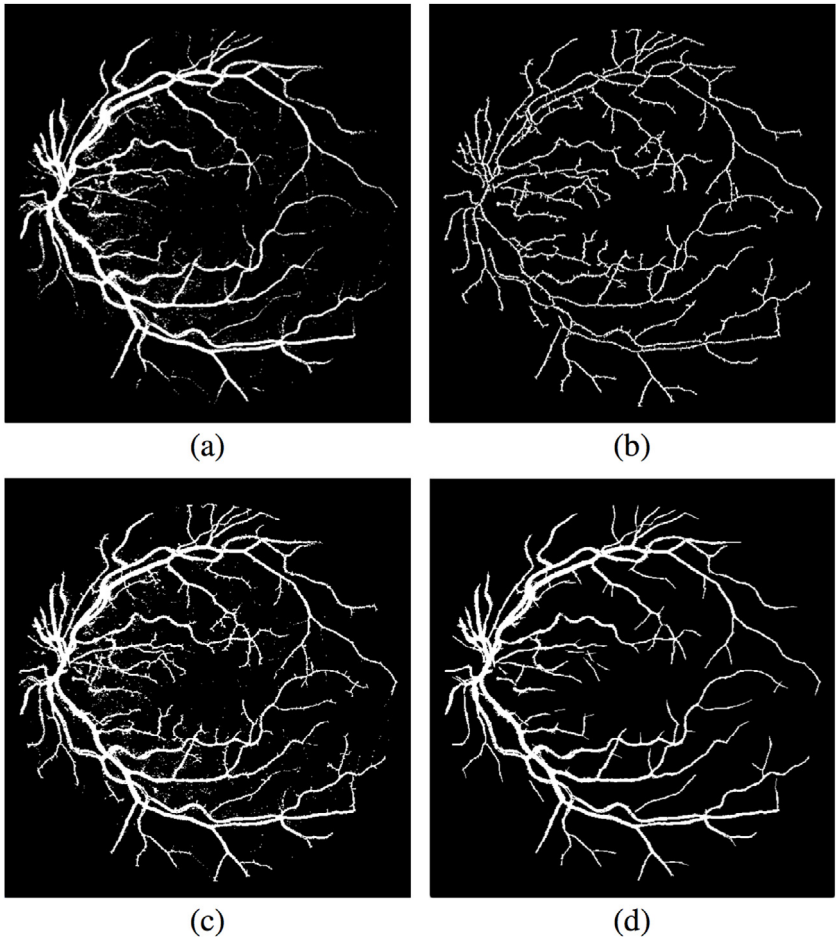

Fig. 7 – Post-processing phase: (a) image after venules structure extraction; (b) image after centerline detection; (c) image after overlapping; (d) the final result of retinal vessel segmentation after de-noising.

4. Result and analysis

In current research, digital retina images for vessel extraction (DRIVE) [4] and structured analysis of the retina (STARE) [17] databases are the most popular ones. Because the retinal images in both DRIVE and STARE databases have fairly good resolution and consistency and contain manually labeled ground truth images which are ideal for training and testing, almost every retinal vessel segmentation research and their performance evaluation are done with these two databases. Since DRIVE provided 40 retinal images, 20 for training while another 20 for testing, we, therefore, used 20 for training the empirical threshold and another 20 for system performance evaluation. As STARE provided 20 labeled images in total, we used 10 for threshold training and another 10 for testing. In this section, our work will be compared to the related ones with three metrics; accuracy (ACC) on the single-database test, accuracy on cross-database test and execution time. We will also look at the sensitivity (SN) and specificity (SP) of each work if provided, where SN reflects the ability of the algorithm to detect the vessel pixels while SP is the ability to detect non-vessel pixels. Those two metrics will be used only to present the feature of a method, but will not be important for performance comparison. Here we have selected the related works with high accuracy or good execution time for comparison.

4.1. *Accuracy on single-database test*

Table 1 illustrates the SN, SP, and ACC of different works, in which the result of Ref. [9] has achieved the highest accuracy of DRIVE database, while the result of Ref. [6] has the top accuracy on STARE. The proposed system has the second highest accuracy on both DRIVE and STARE. However, to verify the reliability of a method, it is expected to be tested on different databases, but Ref. [9] is developed and tested only on DRIVE database, thus causing its result less competitive. The most competitive work to our proposed work is Ref. [6], whose ACC on single database test is slightly better than ours, especially on STARE database. Nonetheless, our proposed system excels this work completely in cross-database test and execution time comparison.

4.2. *Accuracy on cross-database test*

Cross-database test which means to train on one dataset while test on another, is the best way to exam the method dependence on the training dataset. The proposed system is not a supervised method in general, but still it utilizes labeled images to train the empirical threshold, so we switch the empirical thresholds trained from DRIVE and STARE and redo the experiment on those two databases. The cross-database test is an important way to know whether the method will be

Table 1 – Performance comparison on single-database test.

	Database	Sensitivity	Specificity	Accuracy
Lupascu et al. [7]	DRIVE	0.72	–	0.9597
Villalobos-Castaldi et al. [9]	DRIVE	0.9648	0.9480	**0.9759**
Fraz et al. [11]	DRIVE	0.7406	0.9807	0.9480
	STARE	0.7548	0.9763	0.9534
Marin et al. [8]	DRIVE	0.7067	0.9801	0.9452
	STARE	0.6944	0.9819	0.9526
Lam et al. [16]	DRIVE	–	–	0.9472
	STARE	–	–	0.9567
Ricci et al. [6]	DRIVE	–	–	0.9595
	STARE	–	–	**0.9646**
Proposed	DRIVE	0.8375	0.9694	0.9597
	STARE	0.7767	0.9705	0.9579

Bold values indicate the best results in the corresponding database tests.

able to maintain a similar performance aside from the training database. As can be seen in Table 2, the accuracy of Ref. [6] on DRIVE has dropped significantly from 0.9595 (in Table 1) to 0.9266, implying the low robustness of the work. From the observation of Table 2, the proposed system has the best ACC on DRIVE and is the second highest on STARE which is slightly lower than that of Ref. [8]. However, our ACC on DRIVE is much higher than that of Ref. [8]. Besides, the execution time of the proposed one excels the listed all in Table 2.

4.3. *Execution time*

The proposed system was tested on a 2.3 GHz Intel Core i7 4850HQ CPU and was executed in both linear model and parallel model. For linear model, the execution time using one core is 4.906 s and the time distribution is shown in Table 3,

from which we found the execution time ratio of capillaries detection over venules structure extraction was approximately 5:1. When executed under the parallel model, capillaries detection was using 3 cores while venules structure extraction was just using 1 core at the same time. Thus, the parallel execution time is 1.677 s and the speedup is 2.925.

Table 2 – Performance comparison on cross-database test.

	Database	Sensitivity	Specificity	Accuracy
Fraz et al. [11]	DRIVE	0.7242	0.9792	0.9456
	STARE	0.7010	0.9770	0.9493
Marin et al. [8]	DRIVE	–	–	0.9448
	STARE	–	–	**0.9528**
Ricci et al. [6]	DRIVE	–	–	0.9266
	STARE	–	–	0.9452
Proposed	DRIVE	0.9159	0.9559	**0.9538**
	STARE	0.6667	0.9813	0.9515

Bold values indicate the best results in the corresponding database tests.

Table 3 – Running time distribution under linear model.

Processing Phase	Execution time (%)
Capillaries detection	69.7%
Venules structure extraction	13.8%
Preprocessing	10.2%
Post-processing	6.2%
Others	0.1%

Table 4 presents the execution time along with the average accuracy of single and cross-database test, from which we can see Refs. [2] and [3] are the fastest in execution time but has relatively low ACCs. Although Ref. [9] has a really high ACC and a short execution time, it is only tested on DRIVE database. Moreover, sine Ref. [16] is an unsupervised algorithm, the results from its single-database test are comparable with ours from the cross-database test. Even though, not only our ACC is a bit higher but also the running time is much shorter.

5. Conclusion and discussion

This paper has proposed an efficient retinal blood vessels segmentation system, which uses morphological processing method to extract venules and applies matched filter algorithm to detect capillaries separately but simultaneously. The proposed system has achieved a high accuracy with a short execution time.

During the process, the system has utilized top-hat transform for greyscale redistribution and global thresholding for dichotomizing vessel and non-vessel elements in the venules extraction phase; meanwhile, the first-order derivative filter has been applied to the retinal image in 18 directions in order to detect vessel centerlines during the capillaries detection phase. In this way, the venules structure has been best depicted while most capillary details have been preserved.

The proposed retinal vessel segmentation system is fast, highly accurate and robust as well, which is unique among all the related works and thus is also ideal for real-life diagnosis. Besides, the low computing complexity of the proposed methodology and the parallel system architecture have accelerated the execution speed.

The current work is based on greyscale image analysis which may leave an irreversible side effect to the process of later segmentation phases. When filtered by green channel, the non-vessel tissues in the retinal images become more similar to blood vessels, and this happens more often to abnormal retinal images. To solve this problem in the future, some verification steps are expected before de-noising phase. The result after overlapping will be compared with the original RGB image in order to eliminate those real noises.

As we mentioned previously in the introduction, in order to make eye examination more accessible to patients, the

Table 4 – Comparison of execution time with single and cross database accuracy.

	Execution time	Accuracy (single-database)	Accuracy (cross-database)	Platform
Krause et al. [3]	1.2 s	0.9468 (DRIVE)	–	NVIDIA Geforce GPU (GTX680)
Villalobos-Castaldi et al. [9]	3 s	0.9759 (DRIVE)	–	Pentium Dual-Core CPU (2 GHz) 4 GB RAM
Lupascu et al. [7]	125 s	0.9597 (DRIVE)	–	Intel Core 2 Duo CPU (3.16 GHz) 3.25 GB RAM
Koukounis et al. [2]	**0.049** s	0.9234 (DRIVE+STARE)	–	Spartan 6 FPGA
Lam et al. [16]	780 s	0.9520 (DRIVE+STARE)	–	Intel Core 2 Duo CPU (1.83 GHz) 2 GB RAM
Fraz et al. [11]	100 s	0.9507 (DRIVE+STARE)	0.9475 (DRIVE+STARE)	Intel Core 2 Duo CPU (2.27 GHz) 4 GB RAM
Marin et al. [8]	90 s	0.9489 (DRIVE+STARE)	0.9488 (DRIVE+STARE)	Intel Core 2 Duo CPU (2.13 GHz) 4 GB RAM
Proposed	1.677 s	**0.9588 (DRIVE+STARE)**	**0.9527 (DRIVE+STARE)**	Intel Core i7 Duo CPU (2.3 GHz) 16 GB RAM

Bold values indicate either the shortest execution time, or the best results in the corresponding database tests.

automated retinal vessel segmentation system is expected to be implemented in hardware, so as to be handy and portable in the future. Based on our experiments, Raspberry Pi is more suitable and realistic to be the implementation platform candidate.

The FPGA platform, although very efficient in execution time and energy consumption, has an extremely high resource utilization for floating-point operation, while our current system is a floating-point operation based software prototype. Therefore, it is impossible to directly migrate the proposed system without losing accuracy. In other words, we will have to use fixed-point operation instead, which leads to accuracy loss. In the work of [2], the retinal blood vasculature segmentation algorithm used integer operation and was implemented on Spartan 6 FPGA. Their execution time reached to 0.049 s per image, but their accuracy was just 92.34%. As medical imaging always requires a super high precision, it is generally unacceptable to trade accuracy for speed. In this case, we are searching for the alternative solution by implementing the proposed system on Raspberry Pi platform. Raspberry Pi, as one of the most popular single-board computer, is famous for its small-size, low-cost, and high-performance, used widely for IoT applications. We have implemented the proposed system on Raspberry Pi 3 Model B in python, and the current execution time takes 67.69 s per image without loosing accuracy.

Acknowledgement

The authors would like to acknowledge financial support from NSERC.

REFERENCES

[1] Fraz MM, Remagnino P, Hoppe A, Uyyanonvara B, Rudnicka AR, Owen CG, Barman SA. Blood vessel segmentation methodologies in retinal images – a survey. Comput Methods Progr Biomed 2012;108(1):407–33. http://dx.doi.org/10.1016/j.cmpb.2012.03.009

[2] Koukounis D, Ttofis C, Papadopoulos A, Theocharides T. A high performance hardware architecture for portable, low-power retinal vessel segmentation. Integr VLSI J 2014;47(3):377–86. http://dx.doi.org/10.1016/j.vlsi.2013.11.005

[3] Krause M, Alles RM, Burgeth B, Weickert J. Fast retinal vessel analysis. J Real-Time Image Process 2013;11(2):413–22. http://dx.doi.org/10.1007/s11554-013-0342-5

[4] Staal J, Abràmoff MD, Niemeijer M, Viergever MA, van Ginneken B. Ridge based vessel segmentation in color images of the retina. IEEE Trans Med Imaging 2005;23 (4):501–9. http://dx.doi.org/10.1109/TMI.2004.825627

[5] Soares JVB, Leandro JJG, Cesar Jr RM, Jelinek HF, Cree MJ. Retinal vessel segmentation using the 2-D Gabor wavelet and supervised classification. IEEE Trans Med Imaging 2006;25(9):1214–22. http://dx.doi.org/10.1109/TMI.2006.879967

[6] Ricci E, Perfetti R. Retinal blood vessel segmentation using line operators and support vector classification. IEEE Trans Med Imaging 2007;26(10):1357–65. http://dx.doi.org/10.1109/TMI.2007.898551

[7] Lupasscu CA, Tegolo D, Trucco E. FABC: retinal vessel segmentation using AdaBoost. IEEE Trans Inf Technol Biomed 2010;14(5):1267–74. http://dx.doi.org/10.1109/TITB.2010.2052282

[8] Marín D, Aquino A, Gegúndez-Arias ME, Bravo JM. A new supervised method for blood vessel segmentation in retinal images by using gray-level and moment invariants-based features. IEEE Trans Med Imaging 2011;30(1):146–58. http://dx.doi.org/10.1109/TMI.2010.2064333

[9] Villalobos-Castaldi FM, Felipe-Riverón EM, Sánchez-Fernández LP. A fast, efficient and automated method to extract vessels from fundus images. J Vis 2010;13(3):263–70. http://dx.doi.org/10.1007/s12650-010-0037-y

[10] Mendonca AM, Campilho A. Segmentation of retinal blood vessels by combining the detection of centerlines and morphological reconstruction. IEEE Trans Med Imaging 2006;25(9):1200–13. http://dx.doi.org/10.1109/TMI.2006.879955

[11] Fraz MM, Remagnino P, Hoppe A, Uyyanonvara B, Rudnicka AR, Owen CG, Barman SA. An ensemble classification-based approach applied to retinal blood vessel segmentation. IEEE Trans Biomed Eng 2012;59(9):2538–48.

[12] Fraz MM, Barman SA, Remagnino P, Hoppe A, Basit A, Uyyanonvara B, Rudnicka AR, Owen CG. An approach to localize the retinal blood vessels using bit planes and

centerline detection. Comput Methods Programs Biomed 2012;108(2):600–16. http://dx.doi.org/10.1016/j.cmpb.2011.08.009

[13] Abdurrazaq I, Hati S, Eswaran C. Morphology approach for features extraction in retinal images for diabetic retinopathy diagnosis. Proceedings of the International Conference on Computer and Communication Engineering 2008, ICCCE08: Global Links for Human Development; 2008. p. 1373–7. http://dx.doi.org/10.1109/ICCCE.2008.4580830

[14] Sofka M, Stewart CV. Retinal vessel centerline extraction using multiscale matched filters, confidence and edge measures. IEEE Trans Med Imaging 2006;25(12):1531–46. http://dx.doi.org/10.1109/TMI.2006.884190

[15] Xu L, Luo S. A novel method for blood vessel detection from retinal images. Biomed Eng Online 2010;9:14. http://dx.doi.org/10.1186/1475-925X-9-14

[16] Lam BSY, Gao Y, Liew AW. General retinal vessel segmentation using regularization-based multiconcavity modeling. IEEE Trans Med Imaging 2010;29(7):1369–81. http://dx.doi.org/10.1109/TMI.2010.2043259

[17] Hoover A, Kouznetsova V, Goldbaum M. Locating blood vessels in retinal images by piecewise threshold probing of a matched filter response. IEEE Trans Med Imaging 2000;19 (3):203–10. http://dx.doi.org/10.1109/42.845178